Growth and pattern of the mammalian neural tube are governed by partially overlapping feedback activities of the hedgehog antagonists patched 1 and Hhip1

Juhee Jeong and Andrew P. McMahon*

Department of Molecular and Cellular Biology, Harvard University, Cambridge, MA 02138, USA
*Author for correspondence (e-mail: amcmahon@mcb.harvard.edu)

Accepted 8 November 2004

Development 132, 143-154
Published by The Company of Biologists 2005
doi:10.1242/dev.01566

Summary

Upregulation of Patched (Ptc), the *Drosophila* Hedgehog (Hh) receptor in response to Hh signaling limits the range of signaling within a target field by sequestering Hh. In vertebrates, *Ptch1* also exhibits ligand-dependent transcriptional activation, but mutants lacking this response show surprisingly normal early development. The identification of Hh-interacting protein 1 (Hhip1), a vertebrate-specific feedback antagonist of Hh signaling, raises the possibility of overlapping feedback controls. We addressed the significance of feedback systems in sonic hedgehog (Shh)-dependent spinal cord patterning. Mouse embryos lacking both *Ptch1* and *Hhip1* feedback activities exhibit severe patterning defects consistent with an increased magnitude and range of Hh signaling, and disrupted growth control. Thus, *Ptc/Ptch1*-dependent feedback control of Hh morphogens is conserved between flies and mice, but this role is shared in vertebrates with *Hhip1*. Furthermore, this feedback mechanism is crucial in generating a neural tube that contains appropriate numbers of all ventral and intermediate neuronal cell types.

Key words: Hedgehog signaling, Patched 1 (Ptch1, Ptc1), Hhip (Hip1), Feedback, Mouse

Introduction

Among different modes of intercellular signaling, a particularly efficient one for tissue patterning is use of morphogens, secreted signaling molecules that form a long-range concentration gradient over a field of cells and elicit different responses depending on the doses of the signal received by target cells (reviewed by Freeman and Gurdon, 2002). As changes in shape or size of a morphogen gradient can perturb multiple cell populations over a wide area, a tight regulation of morphogen distribution is essential. In addition, the system must be rendered relatively insensitive to fluctuating levels of ligand for a robust outcome.

One important regulatory strategy used in many morphogen systems is negative feedback, where signal transduction leads to upregulation of inhibitors of the pathway to attenuate signaling (Perrimon and McMahon, 1999; Freeman, 2000). Hedgehog (Hh) family proteins, which are important morphogens in both vertebrate and invertebrate development, use such feedback regulation where the inhibitor is actually the Hh receptor, Patched (Ptc), a twelve-pass transmembrane protein (reviewed by Ingham and McMahon, 2001). Ptc is a negative regulator of the Hh pathway that exerts its effects in two different ways: In the absence of Hh, Ptc inhibits activity of Smoothened (Smo), a downstream activator of the pathway. Binding of Hh to Ptc abrogates this repression on Smo, allowing Smo-mediated signal transduction and altered expression of target genes by controlling activities of the transcriptional effector, Cubitus interruptus (Ci). One of the genes upregulated by Hh signaling is *Ptc* itself, and thus *Ptc* is expressed at high levels in the Hh target field close to the source of the ligand (Hooper and Scott, 1989; Nakano et al., 1989). Here, Ptc displays its second function, namely, to sequester Hh (Chen and Struhl, 1996). Studies in *Drosophila* have established that feedback-mediated upregulation of *Ptc* is dispensable for ligand-independent antagonism (LIA), the inhibition of Smo, but is essential for ligand-dependent antagonism (LDA) that results from Hh sequestration. In this study, a transgene expressing a low basal level of Ptc from a heterologous promoter was sufficient to replace endogenous *Ptc*-mediated LIA to Smo activity, but failed to restrain the range of Hh signaling in the responding tissues, indicating that LDA was abolished. LDA limits the range over which the ligand can diffuse, and thus sharpens the morphogen gradient (Chen and Struhl, 1996).

Many features of Hh signaling are conserved between *Drosophila* and mouse, including the fact that Ptch1, the mammalian Hh receptor, is a transcriptional target of the pathway (Goodrich et al., 1996). The role of Ptch1-mediated feedback antagonism during mouse development has been tested in an experiment analogous to the *Drosophila* experiment described above; $Ptch1^{-/-}$ embryos, which die around E8.5 with widespread activation of Hh pathway because of loss of LIA, were provided with a transgene that ubiquitously expresses Ptch1 at low levels from a metallothionein promoter (*MtPtch1*) (Goodrich et al., 1997; Milenkovic et al., 1999). This transgene was expected to restore LIA but not LDA, as the transgene is not responsive to

Hh signaling. Surprisingly, the resulting embryos (*MtPtch1;Ptch1*$^{-/-}$) exhibited a grossly normal body plan both externally and internally at E14.5, a result apparently at odds with Ptch1 playing a significant role in LDA of Hh signaling in the mouse.

Unlike *Drosophila*, vertebrates have several Hh-binding proteins that are transcriptionally regulated by Hh signaling; patched 2 (*Ptch2*) and Hh-interacting protein 1 (*Hhip1*) are positively regulated, whereas growth arrest specific gene 1 (*Gas1*) is negatively regulated (Carpenter et al., 1998; Motoyama et al., 1998; Chuang and McMahon, 1999; Lee et al., 2001). The role of *Ptch2* or *Gas1* in Hh-mediated patterning processes during normal development has yet to be established. Overexpression and loss-of-function studies in the mouse indicate that Hhip1, a cell-surface glycoprotein, is an antagonist of Hh signaling; *Hhip1*$^{-/-}$ embryos die soon after birth, owing to lung defects indicative of overactive Hh signaling (Chuang and McMahon, 1999; Chuang et al., 2003). However, other parts of the body where Hh signaling plays important roles, e.g. the limb, face and spinal cord, develop normally in *Hhip1* mutants. Taken together, the mild phenotypes of both *MtPtch1;Ptch1*$^{-/-}$ and *Hhip1*$^{-/-}$ embryos suggest that Ptch1 and Hhip1 may be functionally redundant in providing feedback LDA to Hh ligands. Consistent with this view, removing one copy of *Ptch1* allele in *Hhip1*$^{-/-}$ embryos (*Hhip1*$^{-/-}$*;Ptch1*$^{+/-}$) causes earlier lethality (around E12.5) and more severe lung and pancreas defects than those observed in *Hhip1*$^{-/-}$ embryos (Chuang et al., 2003; Kawahira et al., 2003).

Although the previous studies point to a role for Ptch1 and Hhip1 in attenuation of paracrine Hh signaling, they did not address the issue of how LDA might contribute to controlling the magnitude (pathway activity at a given position in the tissue) or range (total distance over which the pathway is activated) of a morphogen signaling gradient to generate a specific pattern. The best evidence for Shh acting as a morphogen comes from studies in the vertebrate spinal cord (reviewed by Jessell, 2000; Briscoe and Ericson, 2001; McMahon et al., 2003). Here, Shh is first produced from the notochord that underlies the neural tube, and directs the formation of floor plate which in turn expresses *Shh*. Shh from these two ventral midline sources forms a concentration gradient along the dorsoventral (DV) axis of the neural tube, and represses (Class I proteins) or induces (Class II proteins) expression of several homeodomain and basic helix-loop-helix transcription factors at different thresholds. Cross-repression between the transcription factors sharing a border further sharpens the boundaries of their territories to define five neural progenitor domains in the ventral half of the spinal cord (from ventral to dorsal, p3, pMN, p2, p1, p0; see Fig. 2A). Finally, cells in each domain differentiate into specific types of neurons (from ventral to dorsal, V3, motoneuron (MN), V2, V1, V0; Fig. 2A) based on the combinations of transcription factors they express. As Hh signaling controls the specification of individual progenitor domains by a direct and dose-dependent mechanism (Marti et al., 1995; Roelink et al., 1995; Ericson et al., 1997; Briscoe et al., 2000; Briscoe et al., 2001; Wijgerde et al., 2002), changes in the expression of progenitor domain-associated transcription factors provide sensitive readouts for any perturbations in the Shh morphogen gradient.

We have investigated the role of negative feedback regulation on Hh signaling in vertebrates by analyzing mouse embryos that lack both *Ptch1* and *Hhip1* feedback mechanisms (*MtPtch1;Ptch1*$^{-/-}$*;Hhip1*$^{-/-}$). Our findings indicate that the LDA mediated by these components plays a crucial role in controlling the magnitude and most likely the range of Shh morphogen signaling.

Materials and methods

Generation of *Hhip1* and *Ptch1* compound mutants

MtPtch1 transgene, *Ptch1* null (*Ptch1*$^{-}$) and *Hhip1* null (*Hhip1*$^{-}$) alleles have been described previously (Milenkovic et al., 1999; Goodrich et al., 1997; Chuang et al., 2003). Embryos with compromised LDA to Hh signaling were generated in crosses of *MtPtch1;Ptch1*$^{+/-}$*;Hhip1*$^{+/-}$×*Hhip1*$^{+/-}$*;Ptch1*$^{+/-}$ or *Hhip1*$^{+/-}$*;Ptch1*$^{+/-}$×*Hhip1*$^{+/-}$. The stages of embryos with different genotypes were matched using size and shape of the hindlimb bud and relative size between maxillary and mandibular arches (E10.5), or by somite numbers (E8.5). For E10.5 embryos, neural tube at the forelimb level was used for analysis; for E8.5 embryos, neural tube at the level of second to fourth somite from the anterior was used for analysis.

Immunofluorescence, in situ hybridization and β-galactosidase staining on neural tube sections

Embryos were fixed in 4% paraformaldehyde in PBS for 2 hours (E10.5) or 0.5 hours (E8.5), washed in phosphate-buffered saline (PBS) three times for 10 minutes each, cryoprotected overnight in 30% sucrose/0.1 M phosphate buffer (pH 7.4) and embedded in OCT compound (Tissue-Tek). Frozen sections were prepared at 10 μm (E10.5) or 12 μm (E8.5). For immunofluorescence analysis, the sections were blocked in 3% bovine serum albumin, 1% heat-inactivated sheep serum, 0.1% TritonX-100 in PBS for 1 hour, and then primary antibodies were applied and sections incubated at 4°C overnight. Secondary antibodies were applied at room temperature for 1 hour. Where indicated, the sections were also stained for nuclei (Topro3, Molecular Probes). The images were collected using a Zeiss LSM510 confocal microscope, and the sizes of domains or the numbers of cells expressing particular markers were measured manually from these images. The antibodies used were as follows: rabbit anti-Olig2 1:5000 (gift of H. Takebayashi), rabbit anti-Nkx6.1 1:3000 (gift of J. Jensen), rabbit anti-En1 1:200 (gift of A. Joyner), rabbit anti-Foxa2 1:4000 (gift of A. Ruiz I Altaba), mouse anti-Evx1/2 1:100 (gift of T. Jessell), rabbit anti-Chox10 1:5000 (gift of T. Jessell), rat anti-Lbx1 1:100 (gift of M. Goulding), mouse anti-Nkx2.2 1:50 (DSHB), mouse anti-MNR2 1:20 (DSHB), mouse anti-Pax7 1:20 (DSHB), mouse anti-Pax6 1:20 (DSHB), mouse anti-Shh 1:25 (DSHB), mouse anti-Lim1/2 1:50 (DSHB), mouse anti-Msx1/2 1:30 (DSHB), and Alexa 488 or 568 goat anti-rabbit, anti-mouse or anti-rat (Molecular Probes). Section in situ hybridization was performed as described previously (Schaeren-Wiemers and Gertin-Moser, 1993). The Sim1 probe was a gift from D. Rowitch. β-Galactosidase staining was performed using X-gal as described (Whiting et al., 1991).

Statistical analysis

Three embryos of each genotype and one section from each embryo (E10.5), or two embryos of each genotype and two sections from each embryo (E8.5) were used for quantifications. For the neuronal precursors in Fig. 4, cells from both sides of the spinal cord were counted even though only the right halves are shown in the figure. Difference between wild type and mutant were analyzed by Student's *t*-test.

Constructs for Ptch1-YFP, Hhip1-YFP, YFP-GPI, and Shh-FLAG

To produce a Ptch1-YFP fusion protein, a *Sal*I restriction site was introduced by PCR into mouse Ptch1 cDNA in pcDNA3.1(–) (gift of

M. Scott) immediately upstream of the stop codon. The entire coding sequence of Ptch1 was released by *Nhe*I-*Sal*I digestion from this construct, and the coding sequence for YFP was obtained by cutting pEYFP-1 (Clontech) with *Sal*I and *Not*I. Both inserts were cloned into pECFP-N1 (Clontech) where the CFP coding sequence was removed by *Nhe*I-*Not*I digestion. The resulting Ptch1-YFP fusion protein has YFP at its C-terminal end. To make a construct for Hhip1-YFP fusion protein, a *Bam*H1 site was introduced into coding sequence of Myc-tagged Hhip1 (Chuang and McMahon 1999) just after the signal peptide cleavage site (signal peptide-myc-BamH1-Hhip1). YFP-coding region with *Bam*H1 site at either end was generated by PCR using pEYFP-1 (Clontech) as a template, and cloned into the *Bam*H1 site in Hhip1. The construct for YFP-GPI was a gift from K. Simons. To make a construct for Shh-FLAG, a *Not*I site was inserted by PCR in Shh coding sequence at the position of amino acid 198 (during normal biogenesis of Shh, post-translational cleavage of the protein occurs between amino acids 198 and 199, and cholesterol is covalently attached to amino acid 198). The resulting vector was cut open with *Not*I and *Bam*H1, whose site is in amino acids 202-203 of endogenous Shh sequence, and filled with oligonucleotides encoding amino acids 191-201 to provide a duplication of amino acids 191-198 before and after the *Not*I site. Finally, oligonucleotides encoding triple FLAG tag (amino acids DYKDHDGDYKDHDIDYLDDDDK) were inserted into the above *Not*I site, resulting in Shh amino acids 1-198–3×FLAG–Shh amino acids 191-437.

Transfection and immunostaining of tissue culture cells

Separate dishes of COS-7 cells were transiently transfected with constructs for Ptch1-YFP, Hhip1-YFP, YFP-GPI or Shh-FLAG using FuGENE6 (Roche) following manufacturer's instruction. The next day, cells were trypsinized and mixed in combinations of Ptch1-YFP + Shh-FLAG, Hhip1-YFP + Shh-FLAG or YFP-GPI + Shh-FLAG, and replated on glass cover slips. After another day of incubation, cells were permeabilized in 3% paraformaldehyde, 0.5% TritonX-100 for 2 minutes, fixed in 3% paraformaldehyde in PBS for 15 minutes, and blocked in 6% bovine serum albumin in PBS for 1 hour. Primary antibody (mouse anti-FLAG M2, Sigma) was applied at a 1:300 dilution for 1 hour, followed by secondary antibody (Alexa 568 goat anti-mouse, Molecular Probes) at 1:400 for 30 minutes. Nuclei were stained with Topro3 (Molecular Probes), and the images were collected using a Zeiss LSM510 confocal microscope.

Results

Loss of feedback antagonism to Hh signaling causes gross abnormalities in the face and central nervous system

To address the role of feedback LDA in Hh signaling, we modulated Ptch1 or Hhip1 dose while maintaining Ptch1-dependent LIA to Smo using an *MtPtch1* transgene (see Introduction) (Milenkovic et al., 1999). At E10.5, *Hhip1*$^{-/-}$ embryos appear indistinguishable from the wild type (Fig. 1A,B). However, removing one allele of *Ptch1* (*Hhip1*$^{-/-}$;*Ptch1*$^{+/-}$) resulted in a variable phenotype wherein 56% (5/9) of the embryos were noticeably enlarged, although normally proportioned (Fig. 1A,C). The remainder had an open brain phenotype, with either a normal body size or moderate overgrowth (data not shown). *MtPtch1;Ptch1*$^{-/-}$ embryos looked grossly normal at E10.5, except for a small overgrowth in the diencephalon (arrow in Fig. 1D). However, 88% (7/8) of *MtPtch1;Ptch1*$^{-/-}$;*Hhip1*$^{+/-}$ embryos displayed either exencephaly or spina bifida, and all of them had hyperplastic first branchial arches (Fig. 1E). Embryos lacking both Ptch1- and Hhip1-mediated LDA (*MtPtch1;Ptch1*$^{-/-}$;*Hhip1*$^{-/-}$) had even more profound defects: the entire brain was open, the eyes were absent and the first branchial arches were severely enlarged (6/6; Fig. 1F). In fact, half of the embryos of this genotype recovered at E10.5 (3/6) were already dead and disintegrating. In order to assess the role of feedback LDA in a systematic and quantitative fashion within the confines of the essential genetic models, we focused our analysis on the developing spinal cord, where Shh-mediated patterning is required for the induction of all ventral neural progenitors by E10.5.

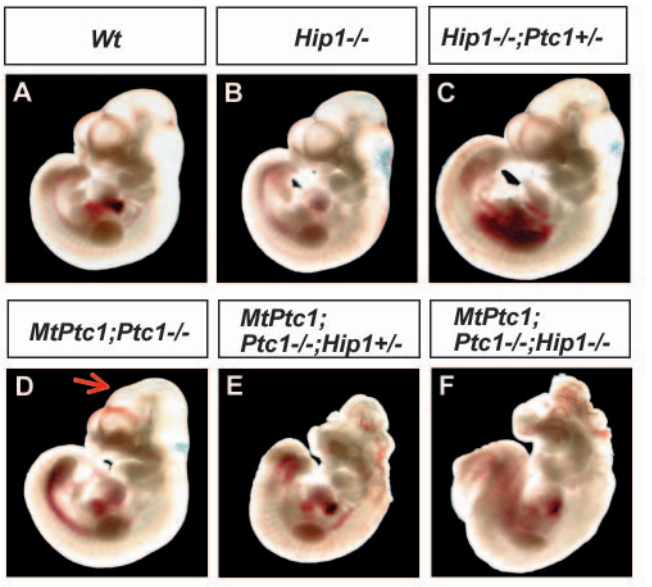

Fig. 1. External features of E10.5 embryos with reduced feedback LDA to Hh signaling. Genotypes are indicated in each panel.

Hhip1$^{-/-}$;*Ptch1*$^{+/-}$ neural tube is overgrown, and shows a moderate expansion of ventral progenitor domains

In the neural tube, both *Ptch1* and *Hhip1* are expressed in response to long-range Shh signaling from floor plate and notochord, covering approximately the ventral half of the neural tube at E10.5 (Goodrich et al., 1996; Chuang and McMahon, 1999). Floor plate was labeled by Foxa2 and Shh (Fig. 2A,D-I), and ventral and dorsal progenitor domains were identified using various combinations of Class II (Nkx2.2, Olig2, Nkx6.1) and Class I (Pax7) transcription factors (Fig. 2A,J-R). For the analyses of ventricular zone at E10.5, we focused on measuring changes in the size of each progenitor domain along the length of the DV axis rather than changes in the cell numbers, which can in fact be a larger difference.

The *Hhip1*$^{-/-}$ neural tube was similar to the wild type in overall size (data not shown), whereas *Hhip1*$^{-/-}$;*Ptch1*$^{+/-}$ neural tube was enlarged, consistent with the increased body size [Fig. 2B,C; neural tube cross-section area: wild type, 0.137 (±0.013) mm^2; mutant, 0.184 (±0.019) mm^2; P=0.062]. Patterning of the ventricular zone was grossly normal in both the *Hhip1*$^{-/-}$ and *Hhip1*$^{-/-}$;*Ptch1*$^{+/-}$ neural tube (Fig. 2D-R); in the latter, both ventral (Fig. 2D-O,S) and dorsal (Fig. 2P-R) cell types were expanded, thus preserving the relative proportions between dorsal and ventral domains to some degree [size of dorsal domain along DV axis: wild type, 45(±4.04) cell diameters; *Hhip1*$^{-/-}$;*Ptch1*$^{+/-}$, 56(±7.37) cell diameters; P=0.053].

However, quantitative analysis revealed a small but statistically significant expansion of ventral progenitor domains in both genotypes (Fig. 2T,U). For example, when the differences in neural tube size are taken into account (Fig. 2U), the domain expressing Nkx6.1 (Nkx6.1^{+}, p3+pMN+p2), which normally occupies 20(±1.08)% of the ventral neural tube, is enlarged to 25.3(±2.25)% (P=0.031) and 29.3(±3.84)% (P=0.033) in *Hhip1*$^{-/-}$ and *Hhip1*$^{-/-}$;*Ptch1*$^{+/-}$ embryos, respectively.

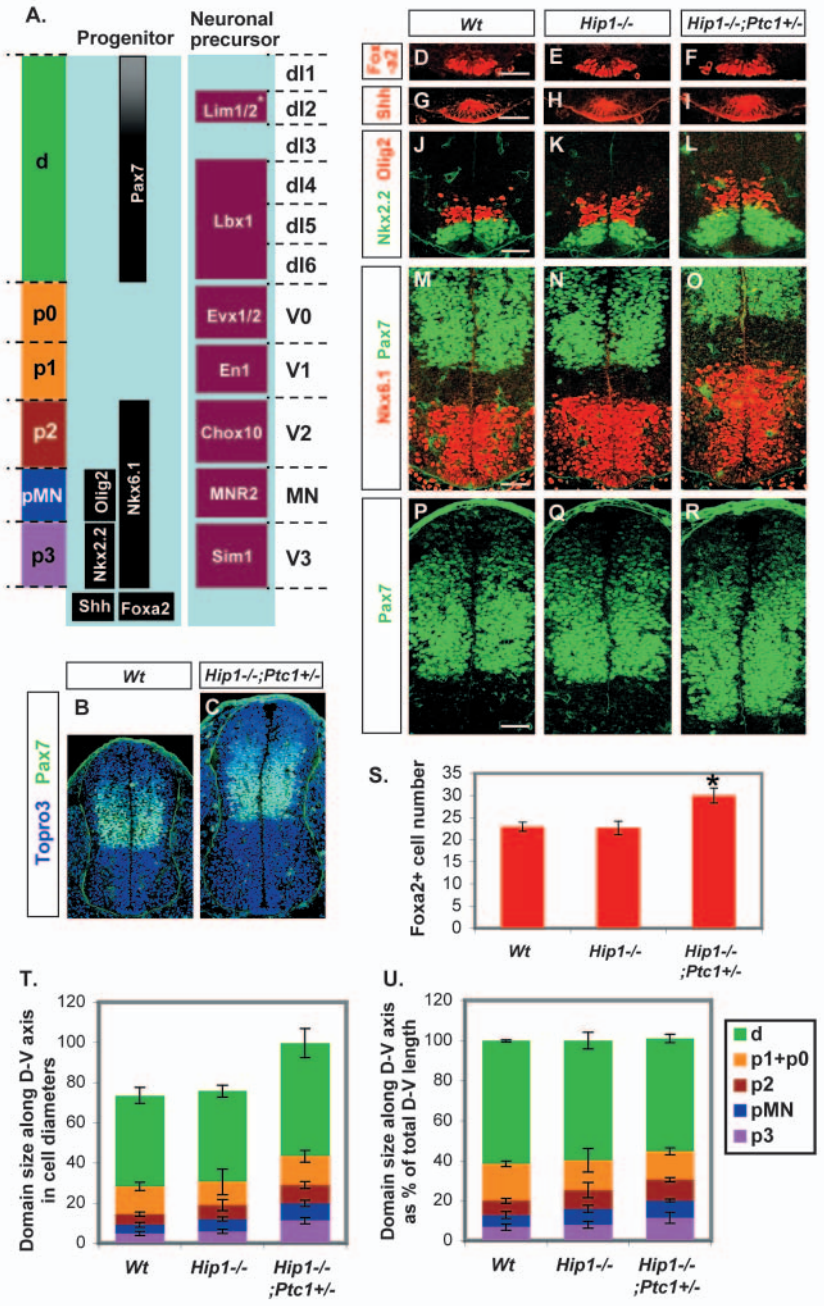

Fig. 2. Growth and patterning phenotypes of *Hhip1*$^{-/-}$ and *Hhip1*$^{-/-}$;*Ptch1*$^{+/-}$ neural tube at E10.5. (A) Summary of the expression patterns of the markers used in this study to identify progenitor domains and neuronal precursor populations (*Lim1/2 has other expression domains more ventrally). (B,C) Cross-sections of neural tube from wild-type (B) and *Hhip1*$^{-/-}$;*Ptch1*$^{+/-}$ (C) embryos. Green, Pax7 protein; blue, nuclei stained with Topro3. (D-R) Immunofluorescence of neural tube sections. Genotypes of the embryos and antibodies as indicated in each panel. Sections in D-O are aligned ventrally (bottom). Sections in P-R are aligned dorsally (top). (S) Quantification of Foxa2^{+} cells in wild type, *Hhip1*$^{-/-}$ and *Hhip1*$^{-/-}$;*Ptch1*$^{+/-}$ embryos (*wild type significantly different from *Hhip1*$^{-/-}$;*Ptch1*$^{+/-}$, P<0.08). (T) Quantification of the size of each progenitor domain along the DV axis in cell diameters in wild-type, *Hhip1*$^{-/-}$ and *Hhip1*$^{-/-}$;*Ptch1*$^{+/-}$ embryos. d, dorsal domain. (U) Representation of the size of each progenitor domain along the DV axis as a percentage of the total DV length of the neural tube. Scale bar: 50 μm.

A complete loss of Ptch1- and Hhip1-mediated LDA leads to a dramatic expansion of ventral progenitor domains, and a reduction of intermediate and dorsal progenitor domains

Next, we examined effects of eliminating Ptch1 component of LDA using *MtPtch1;Ptch1*$^{-/-}$ embryos. In their neural tube, we observed a 2.9-fold expansion of Nkx2.2^{+} p3 domain [Fig. 3I,J,Z; size of p3 along D-V axis: wild type, 5(±1) cell diameters; mutant, 14(±3.5) cell diameters; P=0.057] and 1.4-fold expansion of the Olig2^{+} pMN domain [Fig. 3I,J,Z; size of pMN along DV axis: wild type, 4(±1.2) cell diameters; mutant, 6(±1) cell diameters; P=0.038], although it had less of an effect in more dorsal region (Fig. 3M,N,Q,R,Z,a). Thus, expression of Ptch1 from *MtPtch1* is not able to fully compensate for the removal of endogenous Ptch1, and an enhanced response is observed in the ventral-most Shh-dependent cell identities. However, removing one copy of *Hhip1* (*MtPtch1;Ptch1*$^{-/-}$;*Hhip1*$^{+/-}$) resulted in a further increase in the size of the p3 domain [Fig. 3I,K,Z; size of p3 along DV axis: wild type, 5(±1) cell diameters; mutant, 17(±1.5) cell diameters; P=0.003]. The most striking patterning defects were observed in *MtPtch1;Ptch1*$^{-/-}$;*Hhip1*$^{-/-}$ embryos. In these mutants, the floor plate was three times larger than that of wild-type embryos (Fig. 3A,D,E,H,Y; number of Foxa2^{+} cells: wild type, 23±1; mutant, 69±39; P=0.172). Furthermore, p3 and pMN domains expanded by 5.3 and 3.2 fold, respectively [Fig. 3I,L,Z; size of p3 along DV axis: wild type, 5(±1) cell diameters; mutant, 27(±5.9) cell diameters; P=0.017; size of pMN along DV axis: wild type, 4(±1.2) cell diameters; mutant, 14(±1.7) cell diameters; P=0.028]. By contrast, the Nkx6.1^{-}/Pax7^{-} p1+p0 domain was reduced by 3.7 fold [Fig. 3M,P,Z; size of p1+p0 along DV axis: wild type, 14(±2.1) cell diameters; mutant, 4(±3.5) cell diameters; P=0.010]. The size of Pax7^{+} dorsal domain was also dramatically decreased, by 3.6 fold (Fig. 3Q,T,Z; size of dorsal domain along DV axis: wild type, 45(±4.0) cell diameters; mutant, 13(±8.7) cell diameters; P=0.007). The dorsalmost cells in the neural tube normally express Msx1/2 in response to BMP signaling from the roof plate and surface ectoderm (Liem et al., 1995). Immunostaining for Msx1/2 proteins indicated that this dorsal signaling is

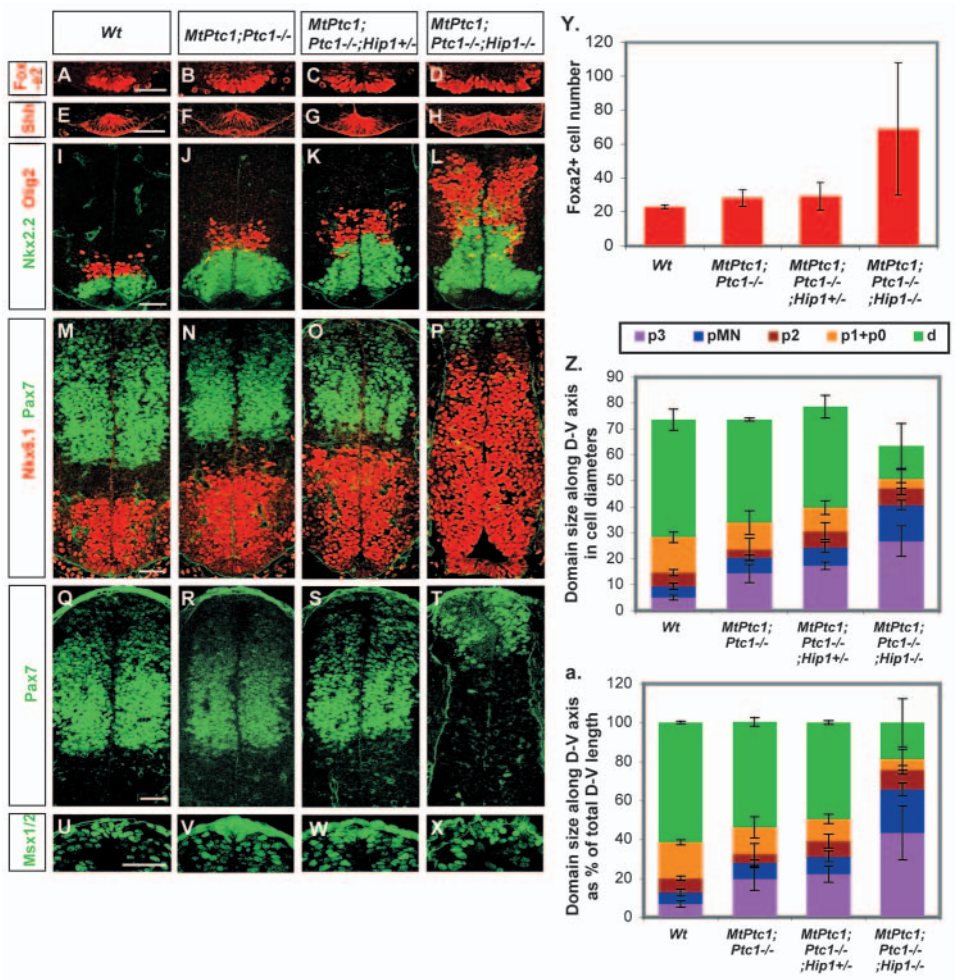

Fig. 3. Patterning phenotypes of the *MtPtch1;Ptch1*$^{-/-}$, *MtPtch1;Ptch1*$^{-/-}$*;Hhip1*$^{+/-}$ and *MtPtch1;Ptch1*$^{-/-}$*;Hhip1*$^{-/-}$ neural tube at E10.5. (A-X) Immunofluorescence of neural tube sections. Genotypes of the embryos and antibodies as indicated in each panel. Sections in A-P are aligned at the same ventral position (bottom). Sections in Q-X are aligned at the same dorsal position (top). (Y) Quantification of Foxa2^{+} cells in wild-type, *MtPtch1;Ptch1*$^{-/-}$, *MtPtch1;Ptch1*$^{-/-}$*;Hhip1*$^{+/-}$ and *MtPtch1;Ptch1*$^{-/-}$*;Hhip1*$^{-/-}$ embryos. (Z) Quantification of the size of each progenitor domain along the DV axis in cell diameters in wild-type, *MtPtch1;Ptch1*$^{-/-}$, *MtPtch1;Ptch1*$^{-/-}$*;Hhip1*$^{+/-}$ and *MtPtch1;Ptch1*$^{-/-}$*;Hhip1*$^{-/-}$ embryos. d, dorsal domain. (a) Representation of the size of each progenitor domain along the DV axis as a percentage of the total DV length of the neural tube. Scale bar: 50 μm.

maintained in even the most extreme genotype, *MtPtch1;Ptch1*$^{-/-}$*;Hhip1*$^{-/-}$ (Fig. 3U-X).

The patterning of wild type, *MtPtch1;Ptch1*$^{-/-}$, *MtPtch1;Ptch1*$^{-/-}$*;Hhip1*$^{+/-}$, and *MtPtch1;Ptch1*$^{-/-}$*;Hhip1*$^{-/-}$ ventricular zones are summarized in Fig. 3Z,a. These data clearly show a stepwise increase in the size of ventral domains (p3 and pMN), and corresponding decrease in the extent of intermediate (p1+p0) and dorsal domains as feedback LDA to Shh is progressively removed from the embryo.

Reduction in intermediate and dorsal neuronal precursors in the neural tube of *MtPtch1;Ptch1*$^{-/-}$*;Hhip1*$^{-/-}$ embryos

We examined whether the changes in neural progenitor domains caused by compromised LDA is reflected by the populations of post-mitotic neuronal precursors. Seven markers were used to identify different neuronal precursor subtypes; in a ventral-to-dorsal progression, these were Sim1 (V3), MNR2 (MN), Chox10 (V2), En1 (V1), Evx1/2 (V0), Lbx1 (dI4+5+6) and Lim1/2 (dI2, dorsal to Lbx1) (Fig. 2A; Fig. 4A,G,M,S).

In *Hhip1*$^{-/-}$ embryos, all seven groups of neuronal precursors were present at normal numbers except for a moderate decrease (37.5%) in V2 cells (Fig. 4A,B,G,H,M,N,S,T,Y-e). However, *Hhip1*$^{-/-}$*;Ptch1*$^{+/-}$ embryos showed a general expansion of neuronal precursor populations (except for dI2), consistent with their proportionally enlarged neural tube reported earlier (Fig. 4C,I,O,U,Y-e).

In *MtPtch1;Ptch1*$^{-/-}$ embryos, the V3 population was twice that of wild-type embryos (Fig. 4A,D,Y; Sim1^{+} area on the section: wild type, 24.7(±3.76) (×100 μm^2); mutant, 48(±5) (×100 μm^2); P=0.003). By contrast, MN, V2, V1, V0 and dI4+5+6 populations did not change significantly (Fig. 4G,J,M,P,S,V,Z-d), but dI2 precursors were reduced by 40% in the absence of Ptch1 LDA [Fig. 4S,V,e; dI2: wild type, 50(±5.3) cells; mutant, 30(±3.5) cells; P=0.003]. A more severe alteration in neuronal precursor populations was observed when *Hhip1* activity was attenuated or removed on this background. In *MtPtch1;Ptch1*$^{-/-}$*;Hhip1*$^{+/-}$ embryos, V3 precursors expanded by 2.2-fold compared with the wild type [Fig. 4A,E,Y; Sim1^{+} area on the section: wild type, 24.7(±3.76) (×100 μm^2); mutant, 55(±4) (×100 μm^2); P=0.001]. The MN population also underwent a 1.5-fold increase [Fig. 4G,K,Z; MN: wild type, 159(±30.4) cells; mutant, 244(±22.1) cells; P=0.031]. By contrast, while V2, V1, V0, and dI4+5+6 precursors were all reduced, these changes were not statistically significant (Fig. 4G,K,M,Q,S,W,a-d). A more severe decrease in dI2 precursors than that observed in *MtPtch1;Ptch1*$^{-/-}$ embryos (2.3-fold fewer than normal) was apparent in the *MtPtch1;Ptch1*$^{-/-}$*;Hhip1*$^{+/-}$ neural tube [Fig. 4S,W,e; dI2: wild type, 50(±5.3) cells; mutant, 21(±7.4) cells; P=0.004].

MtPtch1;Ptch1$^{-/-}$*;Hhip1*$^{-/-}$ embryos showed the most striking changes in neuronal precursor populations, as expected from their severe defects in progenitor domain patterning. V3 precursors in these mutants were increased by 2.3 fold compared with wild-type embryos [Fig. 4A,F,Y; V3: wild type, 24.7(±3.76) (×100 μm^2); mutant, 57(±2) (×100 μm^2); P=0.010]. The MN population was not significantly different from the wild type (Fig. 4G,L,Z). However, V2 precursors

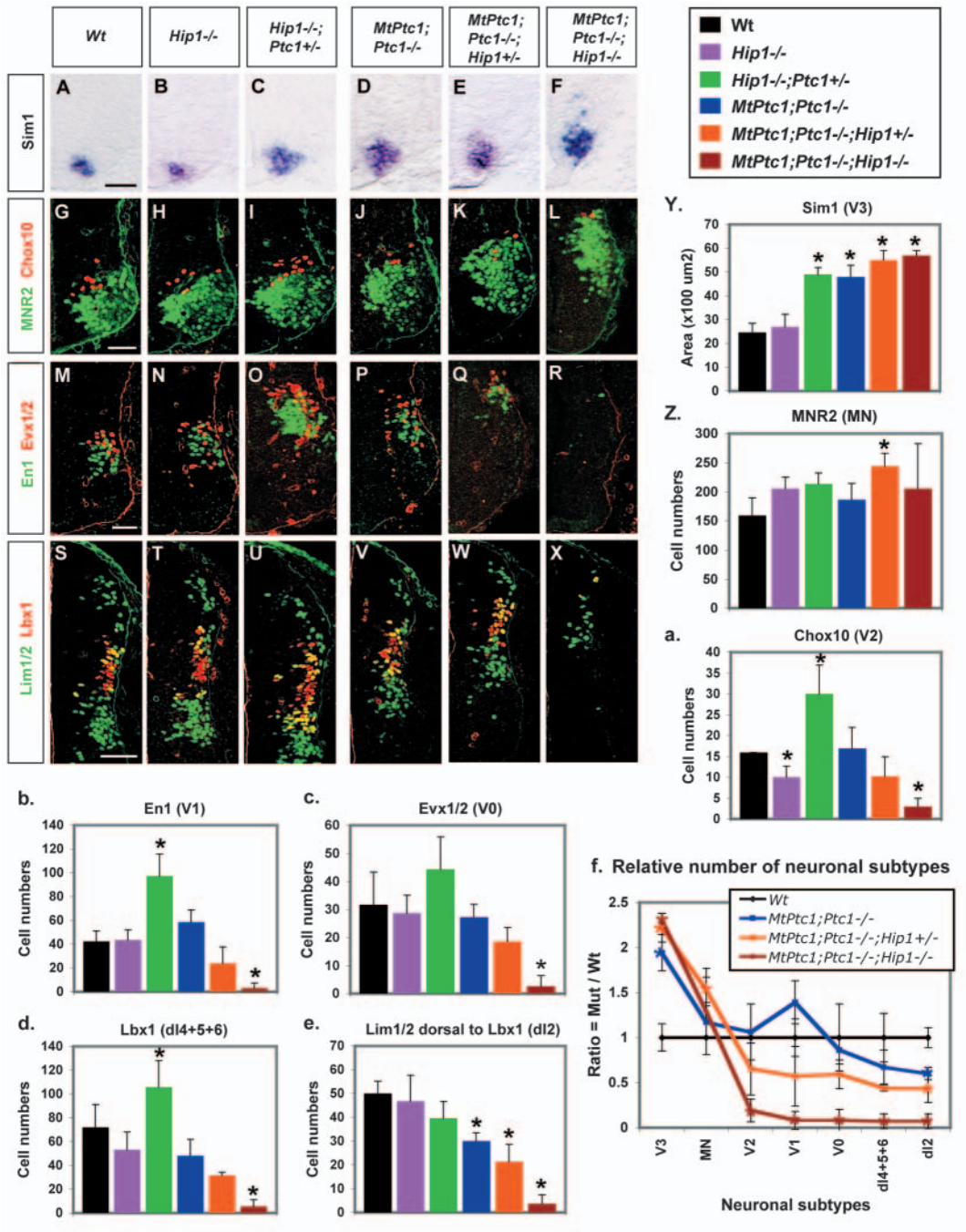

Fig. 4. Changes in ventral and dorsal neuronal precursor populations at E10.5 following disruption of LDA. (A-F) In situ hybridization detection of *Sim1* expression in neural tube sections. Genotypes of the embryos as indicated in each panel. (G-X) Immunofluorescence of neural tube sections. Genotypes of the embryos and antibodies as indicated in each panel. Sections in A-R are aligned ventrally (bottom). Sections in S-X are aligned dorsally (top). (Y-e) Quantification of neuronal precursor populations. (*wild type significantly different from mutant, $P<0.08$). (f) The numbers of different types of neuronal precursors in *MtPtch1;Ptch1*$^{-/-}$, *MtPtch1;Ptch1*$^{-/-}$*;Hhip1*$^{+/-}$ or *MtPtch1;Ptch1*$^{-/-}$*;Hhip1*$^{-/-}$ spinal cord compared with those in the wild type (*wild type significantly different from mutant, $P<0.08$). Scale bar: 50 μm.

were reduced by 5.3 fold [Fig. 4G,L,a; V2: wild type, 16(±0) cells; mutant, 3(±2) cells; P=0.008], and intermediate (V1, V0) and dorsal (dI4+5+6, dI2) neuronal precursors were all present at less than 10% of their normal numbers [Fig. 4M,R,S,X,b-e; V1: wild type, 42(±9.0) cells; mutant, 3(±4.2) cells; P=0.016; V0: wild type, 32(±11.7) cells; mutant, 3(±3.8) cells; P=0.076; dI4+5+6: wild type, 72(±19.3) cells; mutant, 5(±6.11) cells; P=0.035; dI2, wild type, 50(±5.29) cells; mutant, 4(±3.8) cells; P=0.003]. Figure 4f shows the relative sizes of neuronal precursor populations among wild type, *MtPtch1;Ptch1*$^{-/-}$, *MtPtch1;Ptch1*$^{-/-}$*;Hhip1*$^{+/-}$ and *MtPtch1;Ptch1*$^{-/-}$*;Hhip1*$^{-/-}$ embryos for the seven groups of neuronal precursors analyzed. Clearly, in the absence of feedback LDA by Ptch1 and Hhip1 (*MtPtch1;Ptch1*$^{-/-}$*;Hhip1*$^{-/-}$), the number of the ventral neuronal precursors (V3) increased, while intermediate (V1, V0) and dorsal (dI4+5+6, dI2) neuronal precursors were almost ablated, a result consistent with the expansion of ventral progenitor domains and corresponding reduction of intermediate and dorsal progenitor domains in this genotype (Fig. 3Z,a).

The basic patterning of the ventral neural tube is specified at early stages by notochord-derived Shh

We originally predicted that even though ligand production is unaltered, removing LDA would result in both enhanced Hh signaling as increased amount of ligand should be available to trigger receptor-mediated signaling, and an increased spatial range of ligand action in the target field. However, one of the

phenotypes we observed in *MtPtch1;Ptch1*$^{-/-}$*;Hhip1*$^{-/-}$ embryos was a threefold increase in size of the floor plate, which itself expresses *Shh*. This raised the possibility that the patterning defects we observed were due to an increase in ligand production, rather than diffusion or availability of Shh.

During embryogenesis, *Shh* is first expressed in the notochord and then signals to the overlying neural tube to induce its own expression in the floor plate. Although it has been recognized that the acquisition of general ventral identity by neural tube cells depends on early Hh signaling from notochord before the floor plate is established (Ericson et al., 1996), the detailed kinetics for each of Shh-mediated patterning events has not been rigorously addressed to date. We examined early stages of neural tube development (E8.5), at the axial level of the second to fourth somite from the anterior end, to determine timing of ventral progenitor domain patterning in relation to induction of *Shh* in the floor plate (Fig. 5). In a mouse embryo, one somite is added approximately every 90-120 minutes, and thus somitogenesis provides a convenient temporal staging mechanism. Expression of *Nkx6.1* and repression of a Class I gene *Pax6* was already evident at the four-somite stage, the earliest time point we examined (Fig. 5M-R). Cells with weak Olig2 production were first identified at the six-somite stage, but the Olig2 level and the number of Olig2-producing cells increased significantly by the eight-somite stage (Fig. 5G-L). Nkx2.2 was present from the eight-somite stage (Fig. 5G-L). Although Foxa2-producing cells were also detected in the eight-somite stage embryo, high-level expression was not evident until the 13-somite stage (Fig. 5A-F). Importantly, while Shh was expressed in the notochord at all stages examined (arrows in Fig. 5A-F), we observed Shh production by the floor plate only at the 16-somite stage (Fig. 5A-F), shortly after high-level Foxa2 expression was established in ventral midline cells (Fig. 5E). These results indicate that the basic organization of ventral neural progenitor domains is set up by the eight- to 10-somite stage as a result of Shh signaling from the notochord, well before *Shh* expression commences in the floor plate. This finding is consistent with previous reports that *Gli2* mutants, which lack a floor plate, preserve all other ventral cell types, although the p3 progenitor number is decreased (Ding et al., 1998; Matise et al., 1998). Furthermore, the results in Fig. 5 suggest that there is a temporal sequence of repression of Class I and activation of Class II genes at the ventral midline in response to Shh signaling that mirrors their concentration thresholds observed in vitro (Ericson et al., 1997; Briscoe et al., 2000).

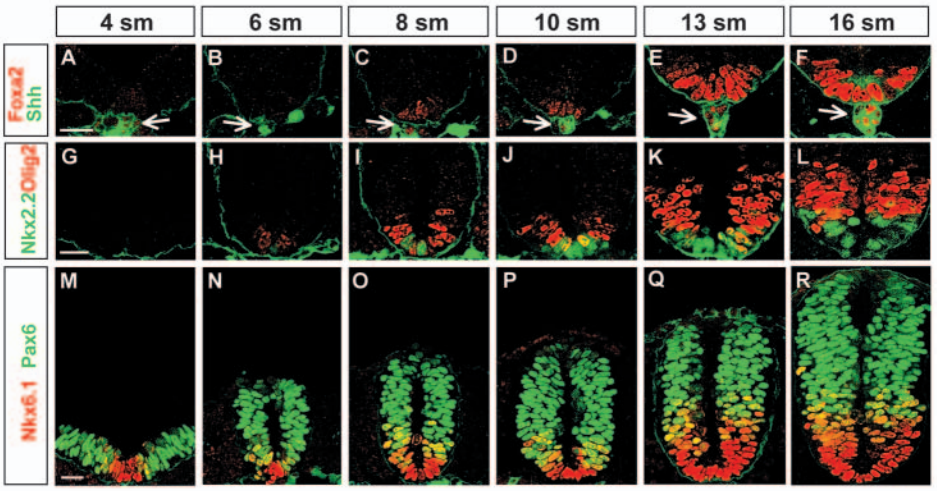

Fig. 5. Shh-dependent patterning in the wild type neural tube around E8.5. (A-R) Immunofluorescence of neural tube sections to assess neural progenitor specification. Stages of the embryos and antibodies as indicated in each panel. Arrows indicate notochord. Scale bar: 25 μm.

The patterning defects in the *MtPtch1;Ptch1*$^{-/-}$*;Hhip1*$^{-/-}$ neural tube are unlikely to be secondary to the enlarged floor plate

Based on the above results, we analyzed neural tube pattern in embryos defective in feedback LDA at the eight- to nine-somite stage to examine primary, notochord-dependent patterning (Fig. 6). As expected, cells producing high level of Shh indicative of floor plate induction were absent from the neural tube in all of the embryos examined at this stage (Fig. 6A-F). However, Foxa2 expression had begun in presumptive floor-plate cells, and their numbers were clearly increased in *MtPtch1;Ptch1*$^{-/-}$ and *MtPtch1;Ptch1*$^{-/-}$*;Hhip1*$^{-/-}$ embryos (Fig. 6A-E). Nkx2.2^{+}, Olig2^{+} and Nkx6.1^{+} populations all increased when LDA to Shh was reduced, in a manner consistent with the observed changes in E10.5 mutants. The neural tube of *Hhip1*$^{-/-}$ mutants appeared normal (Fig. 6A,B,G,H,M,N,Y), but *Hhip1*$^{-/-}$*;Ptch1*$^{+/-}$ embryos showed a moderate patterning defect with a 34% increase in Nkx6.1^{+} cells compared with the wild type [Fig. 6C,I,O,Y; Nkx6.1^{+} (=p3+p3/pMN+pMN+p2): wild type, 28(±2.49) cells; mutant, 37(±2.22) cells; P=0.02]. In the *MtPtch1;Ptch1*$^{-/-}$ neural tube, p3 and pMN populations increased by 1.8- and threefold, respectively [Fig. 6D,J,P,Y; p3 (Nkx2.2^{+}): wild type, 5(±0.58) cells; mutant, 9(±2.08) cells; P=0.03; pMN (Olig2^{+}): wild type, 11(±0.82) cells; mutant, 33(±6.4) cells; P=0.005]. In the complete absence of Ptch1- and Hhip1-mediated feedback LDA (*MtPtch1;Ptch1*$^{-/-}$*;Hhip1*$^{-/-}$), cells that are either Nkx2.2^{+} or Olig2^{+} made up 66% of the entire neural tube compared with 17.5% in wild type (P=0.0003) (Fig. 6K,Y,Z), and Nkx6.1^{+} cells extended up to the dorsal midline (Fig. 6Q). By contrast, the Pax6^{+} domain was reduced significantly in this genotype, and Pax6 and Nkx6.1 were co-expressed in many cells, unlike in the wild type where the co-expression was restricted to a few cells at the Nkx6.1^{+}/Pax6^{+} boundary [Fig. 6M,Q,Y; p1+p0+d (Pax6^{+}Nkx6.1^{-}): wild type, 68(±6.73) cells; mutant, 24(±6.95) cells; P=0.003]. The neural tube patterning phenotypes of LDA mutants at E8.5 are summarized in Fig. 6Y and Fig. 6Z. We conclude that the expansion of ventral progenitor domains in *MtPtch1;Ptch1*$^{-/-}$*;Hhip1*$^{-/-}$ embryos happens prior to increased Shh production from an enlarged floor plate, and therefore reflects enhanced signaling by notochord-derived Shh.

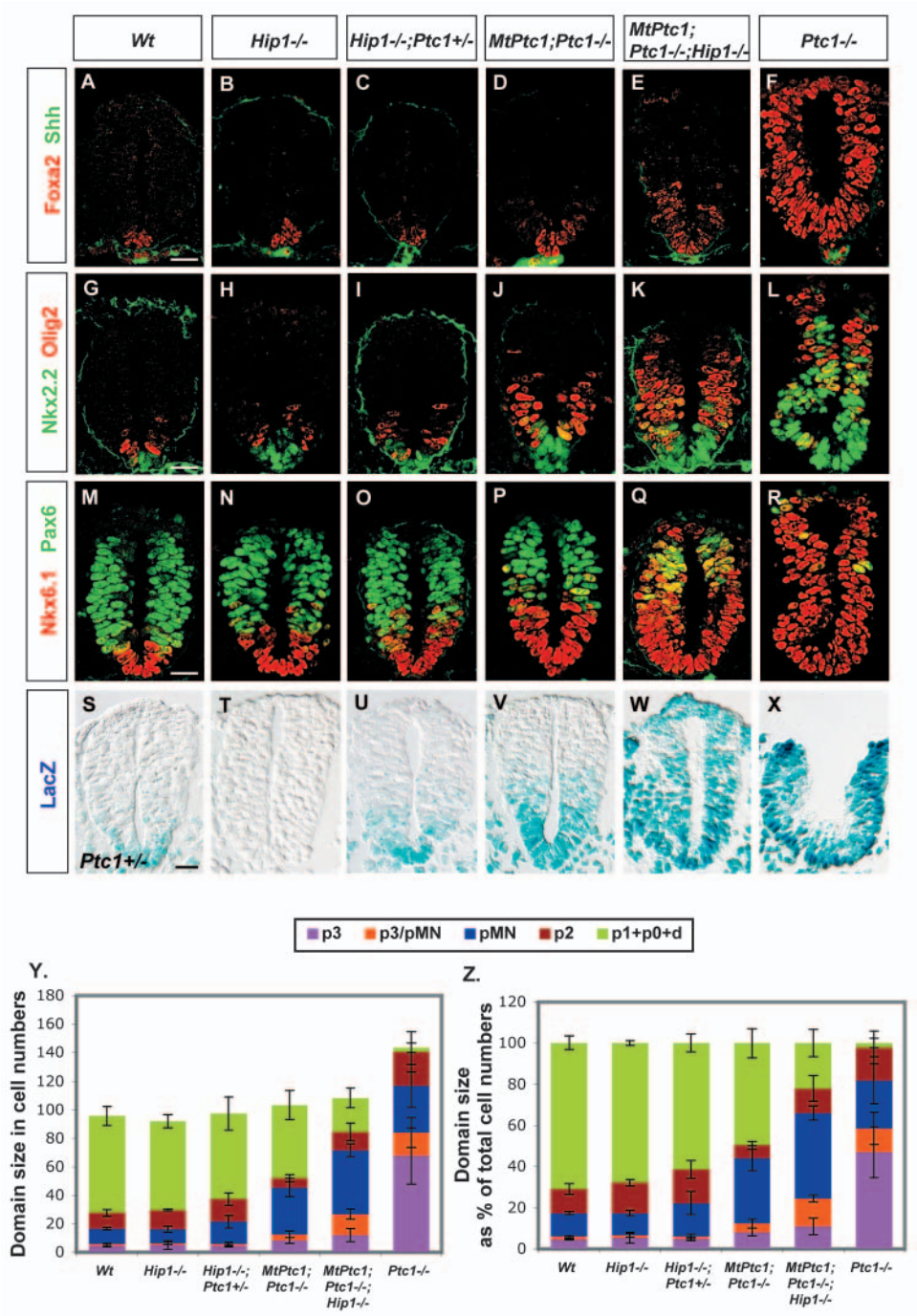

Fig. 6. Neural progenitor domain patterning of feedback LDA mutants at E8.5. (A-R) Immunofluorescence of neural tube sections from eight-to nine-somite stage embryos. Antibodies and genotypes of the embryos as indicated in each panel. (S-X) Analysis for β-galactosidase activity in neural tube sections from 11- to 12-somite stage embryos. The *Ptch1*-null allele has the coding sequence for nucleus-localized β-galactosidase inserted under the *Ptch1* endogenous promoter (Goodrich et al., 1997), and the *Hhip1* null allele has the coding sequence for cytoplasmic β-galactosidase placed under the regulation of *Hhip1* promoter (Chuang and McMahon, 1999), allowing both to serve as potential reporters of Hh signaling. However, as shown in T, the level of β-galactosidase expression from the $Hhip1^{LacZ}$ allele appears to be below the level of detection, suggesting that the staining observed in U and W is predominantly from $Ptch1^{LacZ}$. (Y) Quantification of the size of each neural progenitor population as reflected by cell numbers in wild type and feedback LDA mutants. p3/pMN, $Nkx2.2^{+}Olig2^{+}$; p1+p0+dorsal domain, $Pax6^{+}Nkx6.1^{-}$. (Z) Representation of the size of each progenitor domain as a percentage of the total cell numbers in the neural tube. Scale bar: 25 μm.

The effects of removing feedback LDA to Hh signaling are different from those of removing LIA to Hh signaling

Despite the severe ventralization of the neural tube in *MtPtch1;*$Ptch1^{-/-}$*;*$Hhip1^{-/-}$ embryos, their phenotype was clearly different from that of $Ptch1^{-/-}$ mutants, in which Ptch1-mediated LIA to Smo has been abolished. For example, Foxa2 protein in *MtPtch1;*$Ptch1^{-/-}$*;*$Hhip1^{-/-}$ neural tube was only detected ventrally close to the notochord, the source of Shh (Fig. 6E), whereas Foxa2 was present at high levels in the entire neural tube of $Ptch1^{-/-}$ embryos with no obvious polarity along the DV axis (Fig. 6F). Expression patterns of Nkx2.2, Olig2, Nkx6.1 and Pax6 also showed more severe defects in $Ptch1^{-/-}$ than in *MtPtch1;*$Ptch1^{-/-}$*;*$Hhip1^{-/-}$ neural tubes (Fig. 6K,L,Q,R). For the most part, all neural progenitors in the $Ptch1^{-/-}$ neural tubes, irrespective of their DV position, co-expressed Foxa2 and Nkx6.1 but not Pax6 (Fig. 6F,L,R). Taken together, these results indicate that loss of LIA causes a distinctly different, more uniform ventralization of the neural tube than is observed in LDA mutants. In $Ptch1^{-/-}$ neural tube, $Olig2^{+}$ cells were largely absent ventrally and restricted to a mostly dorsal $Nkx2.2^{-}$ domain (Fig. 6L). This residual DV polarity in progenitor domain pattern is probably due to the influence of signals from the dorsal end (see Discussion).

In the *Ptch1*-null allele, *E. coli lacZ* gene encoding β-galactosidase (β-gal) was placed under the endogenous *Ptch1* promoter, providing a reporter for Hh pathway activation ($Ptch1^{LacZ}$) (Goodrich et al., 1997). In the $Ptch1^{+/-}$ neural tube, which is phenotypically wild type, β-gal activity was present in cells at the ventral end and tapered off in dorsal cells, probably reflecting a normal Shh morphogen gradient (Fig. 6S) (Goodrich et al., 1997). In the $Ptch1^{-/-}$ neural tube, a uniform high-level of β-gal activity along the entire DV axis indicated that ubiquitous, ligand-independent activation of Hh pathway was occurring (Fig. 6X) (Goodrich et al., 1997). However, the introduction of an *MtPtch1* transgene onto this background (*MtPtch1;*$Ptch1^{-/-}$)

eliminated ectopic *Ptch1*^{lacZ} expression in the dorsal half of the neural tube and restored the DV gradient of staining although the stained domain was expanded (Fig. 6V). Thus, *MtPtch1*-mediated LIA was clearly sufficient to block Hh pathway activation where there was no ligand, and the enhanced Hh signaling observed in the ventral half of the neural tube reflects a compromise in LDA. When both Ptch1- and Hhip1-mediated LDA were removed (*MtPtch1;Ptch1*$^{-/-}$*;Hhip1*$^{-/-}$), β-gal expression extended along the entire DV axis of the neural tube (Fig. 6W), but unlike the expression in *Ptch1*$^{-/-}$ embryos, where β-gal activity was uniform, a ventral (high) to dorsal (low) gradient of β-gal activity was retained in the *MtPtch1;Ptch1*$^{-/-}$*;Hhip1*$^{-/-}$ neural tube. As it is very likely that all Hh signaling in the *MtPtch1;Ptch1*$^{-/-}$*;Hhip1*$^{-/-}$ neural tube is ligand dependent (see Discussion), the extent of β-gal and Nkx6.1 expression (Fig. 6Q,W) provides compelling evidence that Shh can travel from the notochord along the entire DV extent of the neuraxis if its movement is not impeded by LDA.

Distinct subcellular localizations of Shh-Ptch1 and Shh-Hhip1 complexes suggest different molecular mechanisms for Ptch1- and Hhip1-mediated LDA

Given their functional overlap in LDA, we examined Ptch1 and Hhip1 activities in cell culture to determine whether both factors use the same mechanism to perform this function. To address this issue, we transfected two populations of COS-7 cells independently with constructs for Ptch1 tagged with yellow fluorescent protein (Ptch1-YFP) and Shh tagged with FLAG epitope (Shh-FLAG), and then mixed the transfected cells on the same dish. We focused our analysis on situations where cells expressing Ptch1-YFP were next to those expressing Shh-FLAG. In these cases, the interaction between the two proteins was not detected at the cell surface (see Fig. S1A,G,M in the supplementary material), but co-localization was observed in intracellular vesicles within Ptch1-YFP producing cells (arrowheads in Fig. S1B,H,N in the supplementary material). These results are consistent with a previous report that Ptch1-mediated LDA appears to remove Shh ligand from the extracellular space by rapid endocytosis, which is probably followed by lysosomal degradation of the ligand (Incardona et al., 2000). In contrast to Ptch1, we observed a strong co-localization of Hhip1-YFP and Shh-FLAG at the cell surface in a similar experiment (see Fig. S1C,I,O in the supplementary material). In particular, we found a strong accumulation of Hhip1-YFP along the edge of the cells abutting those expressing Shh-FLAG (see Fig. S1 in the supplementary material). A small amount of Shh-FLAG was also found in intracellular vesicles in Hhip1-YFP expressing cells, where the two proteins co-localized (arrowheads in Fig. S1D,J,P in the supplementary material), but this was a very minor fraction compared with the level of proteins on the cell surface. A control heterologous cell surface protein (YFP with glycosylphosphatidylinositol (GPI) anchor) did not colocalize with Shh either on the cell surface (see Fig. S1E,K,Q in the supplementary material) or intracellularly (see Fig. S1F,L,R in the supplementary material). Thus, Hhip1 may prevent interaction of Shh with its receptor by sequestering ligand at the cell surface. Endocytosis of Hhip1 and Shh complex, albeit slow, may ultimately remove some ligand-Hhip1 complexes.

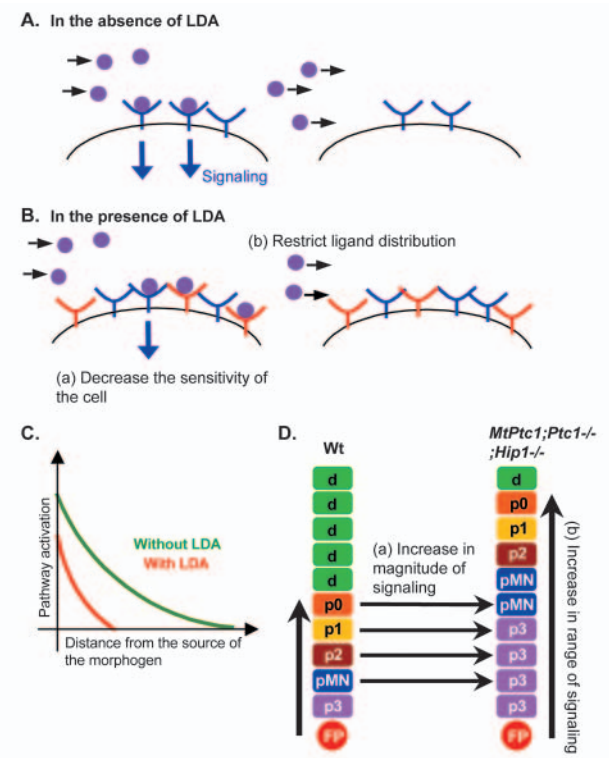

Fig. 7. Model for the regulation of morphogen signaling by LDA. (A) In the absence of LDA, the morphogen (pink circle) produced from a restricted area of the tissue will travel over a field of cells. When the morphogen molecules run into a cell that expresses a signal-transducing receptor (blue cell surface molecule), some of them will bind to the receptor to induce signal transduction (blue arrows), while the rest will move on to the next cell to form a concentration gradient. (B) In the presence of LDA, the antagonists (red cell surface molecule) will compete with the signal-transducing receptors for a limited amount of ligand, and thus decrease the pathway activity within a cell (one blue arrow instead of two in A) at a given concentration of morphogen (cell-autonomous effect). In addition, as the ligands will bind to both receptors and antagonists, less of them will move on to the next cell, which will affect morphogen distribution in the tissue (non-cell autonomous effect). (C) Cell-autonomous and non-cell autonomous effects of LDA together will decrease the magnitude and range of the morphogen signaling gradient. (D) The neural tube patterning defects of *MtPtch1;Ptch1*$^{-/-}$*;Hhip1*$^{-/-}$ embryos are in agreement with the model in A-C (see text).

Discussion

Function of feedback LDA in modulating Shh morphogen signaling

We have investigated the role of Ptch1 and Hhip1 as negative feedback regulators of the Hh pathway in the mammalian neural tube. Both factors participate in LDA, which we define as a mechanism that acts on the ligand at the cell surface to inhibit its function either by sequestering, modifying or degrading that ligand. In general terms, there are two predicted effects for LDA in a target field. First, LDA is expected to decrease the sensitivity of a cell to a given concentration of ligand, as the antagonists will compete with the signal-transducing receptor for a limited amount of ligand (Fig. 7A,B). In this situation, LDA should act cell-autonomously. Second, the antagonists create additional ligand-binding sites

on the cell surface that will interfere with the extracellular movement of the ligand. Therefore, LDA is predicted to restrict the ligand distribution in a tissue, and disruption of LDA in one cell is likely to have non cell-autonomous consequences in the target field (Fig. 7A,B). Together, these two properties would combine to reduce both the magnitude and range of morphogen signaling where LDA is active (Fig. 7C).

Our observation of *MtPtch1;Ptch1*$^{-/-}$*;Hhip1*$^{-/-}$ embryos provides strong evidence for this model; in the ventral half of the neural tube, many cells adopted more ventral fates than expected for their relative DV position along the neuraxis, indicating that Hh pathway activity was abnormally heightened in these cells [Fig. 7D, part a). In addition, the total range of Shh signaling in these mutants, shown by *Ptch1*^{LacZ} reporter or *Nkx6.1* induction, was extended to encompass the entire DV extent of the neural tube. These striking phenotypes of *MtPtch1;Ptch1*$^{-/-}$*;Hhip1*$^{-/-}$ spinal cord underscore the importance of feedback LDA in controlling both the magnitude and range of Shh signaling (Fig. 7D). Two arguments support the assumption that the Hh signaling in *MtPtch1;Ptch1*$^{-/-}$*;Hhip1*$^{-/-}$ neural tube is indeed reflective of the presence of the ligand. First, *Ptch1*^{LacZ} reporter expression showed that LIA is intact in *MtPtch1;Ptch1*$^{-/-}$ embryos, whereas the ubiquitous and strong activation of the Hh pathway in the *Ptch1*$^{-/-}$ neural tube indicates that Ptch1 is the key regulator of LIA, and Hhip1 plays no role in this activity. Given this fact, LIA in *MtPtch1;Ptch1*$^{-/-}$*;Hhip1*$^{-/-}$ embryos should be equivalent to that of *MtPtch1;Ptch1*$^{-/-}$ embryos, and the observed changes in ventral specification in the former reflect attenuated LDA. Second, the progenitor domains in *MtPtch1;Ptch1*$^{-/-}$*;Hhip1*$^{-/-}$ neural tube maintain their normal relative positions, and *Ptch1*^{LacZ} reporter activity also retains a ventral to dorsal gradient. This is consistent with the idea that they are induced by Shh emanating from the ventral midline sources and thus ventral pattern has a vector that reflects a ventral to dorsal movement of Shh ligand.

That a feedback control influences movement of Shh in the neural tube has been postulated from other approaches. When clones of cells that were unable to transduce Hh signal were introduced in the ventral neural tube, cells just dorsal to these clones showed signs that they were exposed to higher levels of Shh than they normally receive (Briscoe et al., 2001; Wijgerde et al., 2002). However, these studies could not specifically address the role of Ptch1 and Hhip1 in LDA, as these clones are unable to express any of the genes that are induced by Hh signaling, among which may be other unidentified antagonists to Shh action.

With regards to the biological significance of LDA in the context of development, removing both Ptch1- and Hhip1-mediated feedback LDA caused a dramatic expansion of ventral progenitors (p3, pMN) at the expense of intermediate (p0+p1) or dorsal progenitors in the neural tube (Fig. 3Z,a). This patterning defect resulted in the generation of an abnormally large number of ventral neurons (V3) and an almost complete lack of intermediate (V1, V0) or dorsal (dI4+5+6, dI2) neurons (Fig. 4f). This result demonstrates that feedback control on Shh signaling by LDA is crucial to the formation of appropriate numbers of all types of ventral and intermediate neurons in the developing spinal cord. Furthermore, the early lethality (around E10.5) and gross abnormalities in the brain and face of *MtPtch1;Ptch1*$^{-/-}$*;Hhip1*$^{-/-}$ embryos suggest that this regulatory mechanism plays important roles in many other regions of the embryo as well.

A recent study using mathematical modeling proposed that the self-enhanced ligand degradation, such as the one resulting from feedback LDA of Ptc (and perhaps Hhip1) to Hh, is essential for robustness of the morphogen gradients to fluctuations in ligand production (Eldar et al., 2003). This prediction can be tested by changing doses of *Shh* allele in embryos with normal or compromised feedback LDA and comparing the changes in the neural tube patterning. For example, differences between the *MtPtch1;Ptch1*$^{-/-}$*;Hhip1*$^{-/-}$ and *MtPtch1;Ptch1*$^{-/-}$*;Hhip1*$^{-/-}$*;Shh*$^{+/-}$ neural tubes are expected to be larger than those between the wild-type and *Shh*$^{+/-}$ neural tubes.

Neural tube patterning defects in the absence of feedback LDA to Shh

In the *MtPtch1;Ptch1*$^{-/-}$*;Hhip1*$^{-/-}$ neural tube, the cell types induced by high levels of Hh signaling, i.e. floor plate, p3 and pMN, all expanded by three- to fivefold, consistent with an overactive Hh pathway in these embryos. However, in the same mutants, p2 progenitor numbers did not change significantly, and p1+p0 progenitors were markedly reduced by almost fourfold. Given that p2 and p1+p0 populations are also directly dependent on and induced by Hh signaling, albeit at lower concentration thresholds than either floor plate, p3 or pMN progenitors, why did they fail to expand (Pierani et al., 1999; Briscoe et al., 2001; Wijgerde et al., 2002)? The answer probably lies in the effects of BMP signals on specification of ventral cell types. BMPs can desensitize ventral neural cells to Shh by interfering with intracellular signal transduction of the Hh pathway (Liem et al., 2000). Furthermore, Dbx1 and Dbx2, two transcription factors that demarcate p1 and p0 domains, are repressed by high levels of BMP signaling (Pierani et al., 1999). In the normal spinal cord, BMPs are expressed at the surface ectoderm and roof plate at the dorsal midline (Liem et al., 1995; Liem et al., 1997), while BMP inhibitors noggin and follistatin are expressed ventrally to counter the actions of BMPs (McMahon et al., 1998; Liem et al., 2000). In *MtPtch1;Ptch1*$^{-/-}$*;Hhip1*$^{-/-}$ embryos, as Shh signaling is enhanced, the low levels of pathway activation appropriate for p2 to p0 fates are likely to occur in a relatively more dorsal position than normal, bringing them close to the dorsal midline (Fig. 3Z). Analysis of Msx1/2 expression indicates that BMP signaling here is intact in *MtPtch1;Ptch1*$^{-/-}$*;Hhip1*$^{-/-}$ embryos (Fig. 3X). Therefore, prospective p2-p0 populations are constrained by too high Hh signaling ventrally and the inhibitory action of BMP signaling dorsally.

The Pax7^{+} dorsal progenitor domain was severely reduced in the *MtPtch1;Ptch1*$^{-/-}$*;Hhip1*$^{-/-}$ neural tube. This result supports the idea that the expansion of ventral cell types we observed was at the expense of dorsal cell fates (i.e. cells that would normally adopt a dorsal fate instead adopted a ventral fate), and argues against an alternative explanation that appropriate numbers of ventral and dorsal neural progenitors were specified initially, but enhanced Hh signaling increased the proliferation rates of ventral cells, causing abnormally rapid expansion of the ventral domains while the dorsal domains grow at the normal rate. In the latter scenario, the size of the dorsal domain in the mutant would remain similar to that

of the wild type. Compelling support for the model of direct specification defects comes from the fact that the severe patterning phenotypes of *MtPtch1;Ptch1*$^{-/-}$*;Hhip1*$^{-/-}$ neural tube were obvious at E8.5 within a few hours of the onset of Shh signaling, insufficient time for a several-fold expansion of a progenitor population by cell proliferation. Furthermore, if the changes in cell proliferation or survival rates were the cause, then the patterning phenotype is expected to get worse as cells go through additional division cycles over the following 2 days. Rather, the ventralization of the mutant neural tube at E8.5 was as severe as it was at E10.5 (compare Fig. 3Z,a and Fig. 6Y,Z).

Mechanism of Ptch1- and Hhip1-mediated LDA to Shh

Although our genetic analysis established that Ptch1 and Hhip1 play overlapping roles in providing LDA to Shh (and most probably other Hh signals in other contexts), the two proteins have very different structures; Ptch1 is a twelve-pass transmembrane protein with two large extracellular loops, a C-terminal cytoplasmic domain and a sterol-sensing domain (SSD), a feature found in several proteins involved in cholesterol homeostasis (Stone et al., 1996; Carstea et al., 1997). By contrast, Hhip1 has one large extracellular domain anchored to the cell membrane by a hydrophobic stretch at the C terminus (Chuang and McMahon, 1999). These differences prompted us to compare the molecular mechanisms that Ptch1 and Hhip1 use to inhibit Shh.

Results herein and those of Incardona et al. (Incardona et al., 2000) suggest that Ptch1 induces rapid endocytosis of Shh, which is followed by degradation of the ligand within the lysosome. As exposing cells that are unable to upregulate Ptch1 expression in response to Hh signal to Hh leads to a significant net decrease in Ptch1 levels on the cell surface, recycling of Ptch1 back to the cell surface, if it occurs, does not seem to be very efficient (Denef et al., 2000). Contrary to Ptch1, our results indicate that Hhip1 appears to inhibit Shh mainly by physically sequestering it at the cell surface, as the ligand is only very inefficiently internalized. This mechanism implies that the antagonism of Hhip1 to Shh is stoichiometric, in line with the copy number-dependent antagonism observed in *MtPtch1;Ptch1*$^{-/-}$, *MtPtch1;Ptch1*$^{-/-}$*;Hhip1*$^{+/-}$ and *MtPtch1;Ptch1*$^{-/-}$*;Hhip1*$^{-/-}$ embryos. However, the endogenous expression level of *Hhip1* appears to be very low, as judged from RNA in situ hybridization or *Hhip1*^{LacZ} reporter staining (Fig. 6T) (Chuang and McMahon 1999), which is unusual for a factor that acts in a stoichiometric fashion. Direct quantitative analysis of Shh and Hhip1 protein levels in the target field, a challenging goal, will be necessary to finally understand this issue.

Growth control by feedback LDA to Hh signaling

Our data that *Hhip1*$^{-/-}$*;Ptch1*$^{+/-}$ embryos had a larger neural tube than wild type implicate feedback LDA in regulation of spinal cord growth. The size of an organ is regulated by controlling both cell death and cell proliferation. In the early neural tube, Shh and Ptch1 have been shown to have anti-apoptotic and pro-apoptotic effects, respectively (Charrier et al., 2001; Thibert et al., 2003). Later in development, Shh acts as a mitogen in several areas of the central nervous system (Rowitch et al., 1999; McMahon et al., 2003). However, we were unable to detect any significant changes in mitosis or apoptosis in *Hhip1*$^{-/-}$*;Ptch1*$^{+/-}$ neural tube compared with the wild type at E10.5 (data not shown). Therefore, it appears that the growth phenotype of these embryos was due to small increase in proliferation or survival rates that had cumulative effects over time.

Importantly, for many of *Hhip1*$^{-/-}$*;Ptch1*$^{+/-}$ embryos, the entire body was overgrown, and this phenotype included an expansion of both ventral Shh-dependent and dorsal Shh-independent cell identities in the neural tube. Although *Ptch1*$^{+/-}$ adult mice were reported to be larger (Goodrich et al., 1997), this was not evident at E10.5 (data not shown). Thus, the growth phenotype of *Hhip1*$^{-/-}$*;Ptch1*$^{+/-}$ clearly implicates Hhip1 as well as Ptch1 in a systemic process that controls body size. This is an intriguing result considering that only a small part of the embryo at E10.5 is subject to Hh signaling and *Hhip1* expression is entirely restricted to cells responding to Hh signals (Chuang and McMahon, 1999). As Hh signaling does not seem to occur in dorsal progenitor domain in *Hhip1*$^{-/-}$*;Ptch1*$^{+/-}$ embryos based on the *Ptch1*^{LacZ} reporter assay (Fig. 6U), enhanced growth in this domain most likely involves some other factors. Further study is necessary to elucidate possible connections between Hh signaling and systemic growth control mechanism in embryonic and adult mouse. In addition, while our data provide unambiguous evidence for combined roles of *Ptch1* and *Hhip1* in LDA during spinal cord patterning, potential interaction of these components with *Ptch2* and *Gas1* remains an unanswered question that will require additional genetic analysis in future studies. Furthermore, new approaches may enable these mechanisms to be addressed in other regions where graded Shh signaling may play a central role in patterning, most notably digit patterning in the vertebrate limb.

We thank H. Takebayashi, J. Jensen, A. Joyner, A. Ruiz i Altaba, T. Jessell, M. Goulding, D. Rowitch, M. Scott, K. Simons and H. Tian for reagents, and M. Wijgerde for sharing his expertise and helpful discussions. This work was supported by a grant to A.P.M. from the NIH (NS33642).

Supplementary material

Supplementary material for this article is available at
http://dev.biologists.org/cgi/content/full/132/1/143/DC1

References

Briscoe, J. and Ericson, J. (2001). Specification of neuronal fates in the ventral neural tube. *Curr. Opin. Neurobiol.* **11**, 43-49.

Briscoe, J., Pierani, A., Jessell, T. M. and Ericson, J. (2000). A homeodomain protein code specifies progenitor cell identity and neuronal fate in the ventral neural tube. *Cell* **101**, 435-445.

Briscoe, J., Chen, Y., Jessell, T. M. and Struhl, G. (2001). A hedgehog-insensitive form of patched provides evidence for direct long-range morphogen activity of sonic hedgehog in the neural tube. *Mol. Cell* **7**, 1279-1291.

Carpenter, D., Stone, D. M., Brush, J., Ryan, A., Armanini, M., Frantz, G., Rosenthal, A. and de Sauvage, F. J. (1998). Characterization of two patched receptors for the vertebrate hedgehog protein family. *Proc. Natl. Acad. Sci. USA* **95**, 13630-13634.

Carstea, E., Morris, J., Coleman, K., Loftus, S., Zhang, D., Cummings, C., Gu, J., Rosenfeld, M., Pavan, W., Krizman, D. et al. (1997). Niemann-Pick C1 disease gene: homology to mediators of cholesterol homeostasis. *Science* **277**, 228-231.

Charrier, J.-B., Lapointe, F., le Douarin, N. M. and Teillet, M.-A. (2001). Anti-apoptotic role of Sonic hedgehog protein at the early stages of nervous system organogenesis. *Development* **128**, 4011-4020.

Chen, Y. and Struhl, G. (1996). Dual roles of Patched in sequestering and transducing Hedgehog. *Cell* **87**, 553-563.
Chuang, P. and McMahon, A. P. (1999). Vertebrate Hedgehog signaling modulation by induction of a Hedgehog-binding protein. *Nature* **397**, 617-621.
Chuang, P., Kawcak, T. and McMahon, A. P. (2003). Feedback control of mammalian Hedgehog signaling by the Hedgehog-binding protein, Hip1, modulates Fgf signaling during branching morphogenesis of the lung. *Genes Dev.* **17**, 342-347.
Denef, N., Neubuser, D., Perez, L. and Cohen, S. (2000). Hedgehog induces opposite changes in turnover and subcellular localization of patched and smoothened. *Cell* **102**, 521-531.
Ding, Q., Motoyama, J., Gasca, S., Mo, R., Sasaki, H., Rossant, J. and Hui, C. C. (1998). Diminished Sonic hedgehog signaling and lack of floor plate differentiation in Gli2 mutant mice. *Development* **125**, 2533-2543.
Eldar, A., Rosin, D., Shilo, B.-Z. and Barkai, N. (2003). Self-enhanced ligand degradation underlies robustness of morphogen gradients. *Dev. Cell* **5**, 635-646.
Ericson, J., Morton, S., Kawakami, A., Roelink, H. and Jessell, T. M. (1996). Two critical periods of Sonic hedgehog signaling required for the specification of motor neuron identity. *Cell* **87**, 661-673.
Ericson, J., Rashbass, P., Schedl, A., Brenner-Morton, S., Kawakami, A., van Heyningen, V., Jessell, T. M. and Briscoe, J. (1997). Pax6 controls progenitor cell identity and neuronal fate in response to graded Shh signaling. *Cell* **90**, 169-180.
Freeman, M. (2000). Feedback control of intercellular signaling in development. *Nature* **408**, 313-319.
Freeman, M. and Gurdon, J. B. (2002). Regulatory principles of developmental signaling. *Annu. Rev. Cell Dev. Biol.* **18**, 515-539.
Goodrich, L. V., Johnson, R. L., Milenkovic, L., McMahon, J. A. and Scott, M. P. (1996). Conservation of the hedgehog/patched signaling pathway from flies to mice: Induction of a mouse patched gene by hedgehog. *Genes Dev.* **10**, 301-312.
Goodrich, L. V., Milenkovic, L., Higgins, K. M. and Scott, M. P. (1997). Altered neural cell fates and medulloblastoma in mouse patched mutants. *Science* **277**, 1109-1113.
Hooper, J. E. and Scott, M. P. (1989). The Drosophila patched gene encodes a putative membrane protein required for segmental patterning. *Cell* **59**, 751-765.
Incardona, J. P., Lee, J. H., Robertson, C. P., Enga, K., Kapur, R. P. and Roelink, H. (2000). Receptor-mediated endocytosis of soluble and membrane-tethered Sonic hedgehog by Patched-1. *Proc. Natl Acad. Sci. USA* **97**, 12044-12049.
Ingham, P. W. and McMahon, A. P. (2001). Hedgehog signaling in animal development: paradigms and principles. *Genes Dev.* **15**, 3059-3087.
Jessell, T. M. (2000). Neuronal specification in the spinal cord: Inductive signals and transcriptional codes. *Nat. Rev. Genet.* **1**, 20-29.
Kawahira, H., Ma, N. H., Tzanakakis, E. S., McMahon, A. P., Chuang, P. and Hebrok, M. (2003). Combined activities of hedgehog signaling inhibitors regulate pancreas development. *Development* **130**, 4871-4879.
Lee, C. S., Buttitta, L. and Fan, C.-M. (2001). Evidence that the WNT-inducible *growth arrest-specific gene 1* encodes an antagonist of sonic hedgehog signaling in the somite. *Proc. Natl. Acad. Sci. USA* **98**, 11347-11352.
Liem, K. F., Jr, Tremml, G., Roelink, H. and Jessell, T. M. (1995). Dorsal differentiation of neural plate cells induced by BMP-mediated signals from epidermal ectoderm. *Cell* **82**, 969-979.
Liem, K. F., Jr, Tremml, G. and Jessell, T. M. (1997). A role for the roof plate and its resident TGFβ-related proteins in neuronal patterning in the dorsal spinal cord. *Cell* **91**, 127-138.
Liem, K. F., Jr, Jessell, T. M. and Briscoe, J. (2000). Regulation of the neural patterning activity of sonic hedgehog by secreted BMP inhibitors expressed by notochord and somites. *Development* **127**, 4855-4866.
Marti, E., Bumcrot, D. A., Takada, S. and McMahon, A. P. (1995). Requirement of 19K form of Sonic hedgehog for induction of distinct ventral cell types in CNS explants. *Nature* **375**, 322-325.
Matise, M. P., Epstein, D. J., Park, H. L., Platt, K. A. and Joyner, A. L. (1998). Gli2 is required for induction of floor plate and adjacent cells, but not most ventral neurons in the mouse central nervous system. *Development* **125**, 2759-2770.
McMahon, J. A., Takada, S., Zimmerman, L. B., Fan, C.-M., Harland, R. M. and McMahon, A. P. (1998). Noggin-mediated antagonism of BMP signaling is required for growth and patterning of the neural tube and somite. *Genes Dev.* **12**, 1438-1452.
McMahon, A. P., Ingham, P. W. and Tabin, C. J. (2003). Developmental roles and clinical significance of Hedgehog signaling. *Curr. Top. Dev. Biol.* **53**, 1-114.
Milenkovic, L., Goodrich, L. V., Higgins, K. M. and Scott, M. P. (1999). Mouse patched1 controls body size determination and limb patterning. *Development* **126**, 4431-4440.
Motoyama, J., Takabatake, T., Takeshima, K. and Hui, C. (1998). Ptch2, a second mouse Patched gene is co-expressed with Sonic hedgehog. *Nat. Genet.* **18**, 104-106.
Nakano, Y., Guerrero, I., Hidalgo, A., Taylor, A., Whittle, J. R. and Ingham, P. W. (1989). A protein with several possible membrane-spanning domains encoded by the Drosophila segment polarity gene patched. *Nature* **341**, 508-513.
Perrimon, N. and McMahon, A. P. (1999). Negative feedback mechanisms and their roles during pattern formation. *Cell* **97**, 13-16.
Pierani, A., Brenner-Morton, S., Chiang, C. and Jessell, T. M. (1999). A Sonic hedgehog-independent, retinoid-activated pathway of neurogenesis in the ventral spinal cord. *Cell* **97**, 903-915.
Roelink, H., Porter, J. A., Chiang, C., Tanabe, Y., Chang, D. T., Beachy, P. A. and Jessell, T. M. (1995). Floorplate and motor neuron induction by different concentrations of the amino terminal cleavage product of Sonic hedgehog autoproteolysis. *Cell* **81**, 445-455.
Rowitch, D. H., St-Jacques, B., Lee, S. M. K., Flax, J. D., Snyder, E. Y. and McMahon, A. P. (1999). Sonic hedgehog regulates proliferation and inhibits differentiation of CNS precursor cells. *J. Neurosci.* **19**, 8954-8965.
Schaeren-Wiemers, N. and Gerfin-Moser, A. (1993). A single protocol to detect transcripts of various types and expression levels in neural tissue and cultured cells: In situ hybridization using digoxigenin labeled cRNA probes. *Histochemistry* **100**, 431-440.
Stone, D., Hynes, M., Armanini, M., Swanson, T., Gu, Q., Johnson, R., Scott, M., Pennica, D., Goddard, A., Phillips, H. et al. (1996). The tumor-suppressor gene patched encodes a candidate receptor for Sonic hedgehog. *Nature* **384**, 129-134.
Thibert, C., Teillet, M.-A., Lapointe, F., Mazelin, L., le Douarin, N. and Mehlen, P. (2003). Inhibition of neuroepithelial Patched-induced apoptosis by Sonic hedgehog. *Science* **301**, 843-846.
Whiting, J., Marshall, H., Cook, M., Krumlauf, R., Rigby, P. W., Scott, D. and Allemann, R. K. (1991). Multiple spatially specific enhancers are required to reconstruct the pattern of Hox-2.6 gene expression. *Genes Dev.* **5**, 2048-2059.
Wijgerde, M., McMahon, J. A., Rule, M. and McMahon, A. P. (2002). A direct requirement for Hedgehog signaling for normal specification of all ventral progenitor domains in the presumptive mammalian spinal cord. *Genes Dev.* **16**, 2849-2864.